бенности сигнала во временной и частотной областях. Идентификацию модальных параметров, которая эффективно достигается с помощью анализа главных компонент (PCA), можно рассматривать как тип системного распознавания.

Результаты. Поскольку метод анализа главных компонент чувствителен к Гауссову шуму при измерениях, в работе предлагается новый метод комбинирования подавления шума на основе вейвлет-преобразования с методом анализа главных компонент, и применяется эта техника в идентификации модальных параметров.

Научная новизна. Сигналы поддаются разложению на вейвлеты с несколькими слоями, а полученные вейвлет-коэффициенты предварительно обрабатываются в соответствии с пороговым значением. Затем они реконструируются с уменьшением влияния шума. Исследования этого аспекта ранее не проводились.

Практическая значимость. Результаты моделирования на примере балок показывают, что предложенный метод способен распознавать основные модальные формы и собственные частоты. Кроме того, он позволяет улучшать точность выявленных модальных параметров и извлекать некоторые ранее упущенные колебания.

Ключевые слова: *идентификация модальных параметров, анализ главных компонент (PCA), Вейвлет-шумоподавление, системы распознавания, вейвлет-анализ, Гауссов шум при измерениях*

Рекомендовано до публікації докт. техн. наук В. В. Гнатушенком. Дата надходження рукопису 27.05.15.

Guoliang Sun

Rongcheng College of Harbin University of Science and Technology, Weihai, China

WAVELET IMAGE DENOISING BASED ON FUSION THRESHOLD FUNCTIONS

Гуолян Сун

Коледж Ронгченг Харбінського університету науки та технології, Вейхай, Китай

ВЕЙВЛЕТ-ФІЛЬТРАЦІЯ ШУМУ В ЗОБРАЖЕННЯХ, ЩО ЗАСНОВАНА НА ЗЛИТТІ ПОРОГОВИХ ФУНКЦІЙ

Purpose. Specific to the existing discontinuity and constant deviation in denoising of wavelet threshold function, this paper analysed the integrated denoising function of traditional wavelet threshold function.

Methodology. Through analysis of the defects of wavelet soft threshold function and hard threshold function and according to the characteristics of the traditional threshold function as well as the design idea and procedure, the paper establishes an integrated threshold function on the basis of the traditional threshold function and offers a simulation diagram extracted from the corresponding threshold function. Through the simulation diagram of the threshold function, it analyses the advantages of integrated threshold function.

Findings. According to the result, the integrated threshold function established on the basis of the characteristics and design idea of wavelet soft threshold function and hard threshold function integrates the advantages of traditional threshold functions, effectively overcoming the discontinuity of the hard threshold function and constant deviation of the soft threshold function.

Originality. Based on the structure and characteristics of the traditional wavelet threshold function, the article puts forward an idea how to combine the traditional wavelet threshold function and the fusion function which is not only used to transform the traditional threshold function, but also adds the fusion coefficient to modify it, which makes the fusion function adaptive.

Practical value. The results of the paper can effectively improve the denoising ability of an image, which apart from effective removal of image noise, reserves detailed information of images, laying solid foundation for in-depth processing of a high-quality image.

Keywords: *wavelet transformation, threshold function, fusion threshold function, image denoising*

Introduction. With the development of information technology, people are more and more dependent on information transmitted by digital images. However, images often have certain noise in the process of transmission and acquisition [1]. Meanwhile, when noise reaches a certain degree, it will blur the characteristics of images and greatly affect the further analysis and application of images [2–3]. Therefore, to make the subsequent image processing go on smoothly, people keep developing all kinds of denoising methods to preprocess images, to obtain better recovered images and satisfy demands of various image applications.

Traditional image denoising methods include two types: spatial domain and frequency domain [4–5]. Typical spatial-domain filters include mean filters and wiener filters. A mean filter signifies each pixel value in

an image with the average of all pixel values in the set neighbourhood of the pixel, while a Wiener filter uses statistical information of spatial domain of an image. It is a classic linear filter based on minimum mean square error and has a good denoising effect on Gaussian noise. However, the aforementioned traditional denoising methods only have a local analytical ability for spatial domain and frequency domain. While suppressing image noise, image edges and other details are lost, which makes the processed image blurred or distorted. It cannot satisfy high requirements of subsequent processing of images.

On the other hand, wavelet transformation based on wavelet domain has a good time-frequency localization property [6]. It can not only remove noises in images effectively, but also retains all details in images simultaneously. Moreover, in the process of wavelet denoising, the structure of threshold function greatly affects its denoising effect. Traditional soft and hard wavelet threshold functions were first presented by Donoho in 1995 [7]. Image denoising on the basis of soft and hard thresholds has also been widely applied in practice and contributes to achieving a good image denoising effect. However, traditional soft and hard wavelet threshold functions still have large material defects [8]. For example, when processing an image with complex noise, the derived image may be subject to distortion and deviation.

For this reason, based on traditional soft and hard wavelet threshold functions, this paper analyses structures and defects of traditional threshold functions. According to the characteristics, design ideas and procedures of traditional threshold functions, this paper presents fusion threshold functions based on traditional wavelet threshold functions and develops new wavelet threshold functions. Through relevant image denoising simulation, the benefits of fusion threshold functions in image denoising are analysed.

Wavelet transformations of two-dimensional images. The data form of images is two-dimensional signals, and multi-resolution analysis of two-dimensional signals is similar to that of one-dimensional and only requires changing the space $L^2(R)$ into $L^2(R*R)$. The scaling function $\varphi(x)$ introduced into one-dimensional signals is also changed into $\varphi(x, y)$.

Suppose $\{V_j\}_{j\in Z}$ is a multi-resolution analytical space of $L^2(R)$. Then we have a multi-resolution analysis of subspace $L^2(R*R)$ constituted by the tensor space $\{V_j^2\}_{j\in Z}$: $V_j^2 = V_j \oplus V_j$. The two-dimensional scaling function $\varphi(x, y)$ of two-dimensional multi-resolution analysis $\{V_j^2\}_{j\in Z}$ is shown in Eq. 1.

$$\varphi(x, y) = \varphi(x)\varphi(y), \quad (1)$$

where $\varphi(x)$ is a one-dimensional scaling function of $\{V_j\}_{j\in Z}$. This equation shows the one-dimensional separability of the two-dimensional scaling function. For each $j\in Z$, the function system $\{\varphi_{j,n,m}(x, y) = \varphi_{j,n}(x)\varphi_{j,m}(y) | (n, m)\in Z^2\}$ constitutes an orthonormal basis of the space $\{V_j^2\}_{j\in Z}$. The calculation of subscripts j, n and m is shown in Eq. 2

$$\varphi_{j,n,m}(x, y) = 2^j\varphi(x - 2^j n)\varphi(y - 2^j m), \quad (j \geq 0), \quad (2)$$

where $\{V_j^2\}_{j\in Z}$ is called a separable multi-resolution space of $L^2(R*R)$. Since both $\varphi(x)$ and $\varphi(y)$ are low-pass scaling functions, the derived $\{V_j^2\}_{j\in Z}$ is a smooth low-pass space.

If $\psi(x)$ is an orthogonal wavelet of one-dimensional multi-resolution analysis $\{V_j\}_{j\in Z}$, then three wavelet functions of two-dimensional multi-resolution analysis are

$$\begin{aligned} \psi^1(x, y) &= \varphi(x)\psi(y); \\ \psi^2(x, y) &= \psi(x)\varphi(y); \\ \psi^3(x, y) &= \psi(x)\psi(y). \end{aligned} \quad (3)$$

For each $j \in Z$, their integer translation systems are

$$\begin{aligned} \psi^1_{j,n,m}(x,y) &= \varphi_{j,n}(x)\psi_{j,m}(y); \\ \psi^2_{j,n,m}(x,y) &= \psi_{j,n}(x)\varphi_{j,m}(y); \\ \psi^3_{j,n,m}(x,y) &= \psi_{j,n}(x)\psi_{j,m}(y). \end{aligned} \quad (4)$$

The superscripts in Eq.4 above are just indices. They form an orthonormal basis of $\{W_j^2\}_{j\in Z}$. Therefore, the above three orthogonal bases contain at least a band pass $\psi(x)$ or $\psi(y)$. So they are all band-pass. In other words, all of these three parts reflect the details. Hence, the function

$$\{\psi^\varepsilon_{j,n,m}(x,y)\} = \{2^j\psi^\varepsilon(x - 2^j n, y - 2^j m\},$$

where $j \geq 0$, $\varepsilon = 1, 2, 3$ is an orthogonal basis of $L^2(R\times R)$. Other parameters are integers. $\varepsilon = 1, 2, 3$ is corresponding to three different directions, i.e., horizontal, vertical and diagonal ones. So for two-dimensional image signal $f(x, y) \in L^2(R\times R)$, at the resolution of 2^{-j}, we have

$$\begin{aligned} A_j f &= \left\langle f(x,y), \varphi_{j,n,m}(x,y)\right\rangle, (n,m)\in Z^2; \\ D_j^1 f &= \left\langle f(x,y), \psi^1_{j,n,m}(x,y)\right\rangle, (n,m)\in Z^2; \\ D_j^2 f &= \left\langle f(x,y), \psi^2_{j,n,m}(x,y)\right\rangle, (n,m)\in Z^2; \\ D_j^3 f &= \left\langle f(x,y), \psi^3_{j,n,m}(x,y)\right\rangle, (n,m)\in Z^2. \end{aligned} \quad (5)$$

The above Eq. 5 shows that at the resolution of 2^{-j}, the image is decomposed into four sub-images, $A_j f$, $D_j^1 f$, $D_j^2 f$ and $D_j^3 f$. Among them, $A_j f$ stands for an approximation of the original image at the resolution of 2^{-j} (i.e., low frequency part of the image, represented as LL). $D_j^\varepsilon f$ stands for an error of such approximation (i.e., high frequency part of the image). $D_j^1 f$ corresponds to the high frequency part in a vertical direction, i.e., horizontal edge (detail) information (represented as LH). $D_j^2 f$ is corresponding to the high frequency part in horizontal direction, i.e., vertical edge (detail) information (represented as HL). While $D_j^3 f$ corresponds to the high frequency part in a diagonal direction (represented as HL). Fig. 1 shows a multi-resolution wavelet decomposition of a two-dimen-

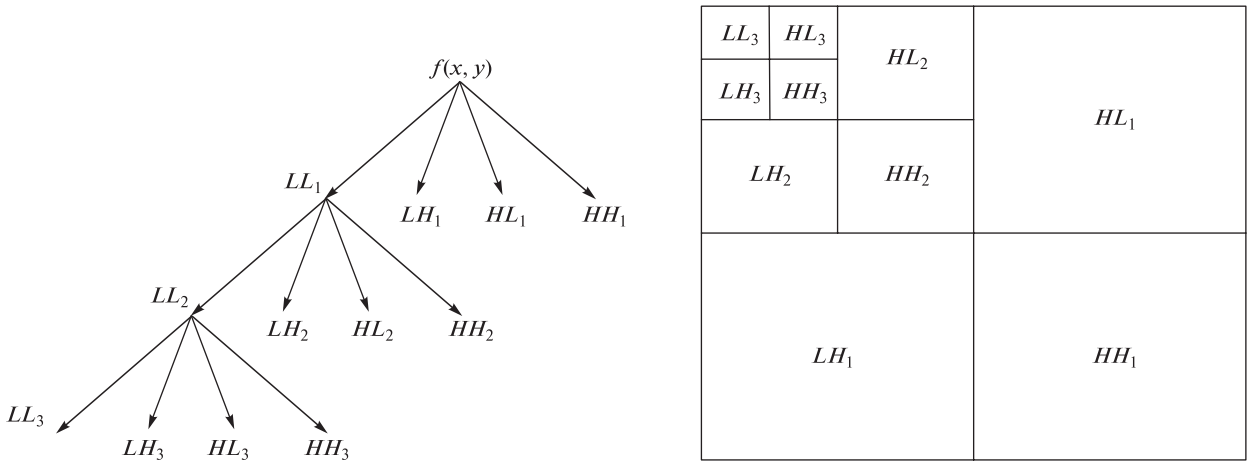

Fig. 1. 3-Level Wavelet Decomposition of a Two-dimensional Image:
a — Wavelet Tree Structure; b — Pyramid Structure of Wavelet Decomposition

sional image vividly, suggestive of 3-level wavelet decomposition of image. The superscripts in the image stand for the number of wavelet decomposition levels. From the image, it can be seen that at every decomposition level, the image is decomposed into four frequency bands: *LL*, *LH*, *HL* and *HH*. At the next level of decomposition, only low frequency component *LL* is decomposed.

Fig. 2 below demonstrates an example of applying different wavelet functions on a two-dimensional picture "Lena" for the purpose of 2-level and 3-level decompositions.

It is obvious from Fig. 2 that decomposed images of different wavelet functions vary and the levels of decomposition of the same wavelet function are also different. From the overall decomposition results, image decomposition using wavelet algorithm can obtain key information in all parts of an image and lay a foundation for further image processing.

Wavelet transformation image denoising based on fusion threshold functions. ***Fused and Optimized Threshold Functions.*** In the process of denoising, a threshold function is actually processing a coefficient derived from wavelet transformation. Therefore, in essence, a threshold function processes signals with noise. A wavelet coefficient corresponding to an image signal contains a lot of important information. It has fewer data and larger amplitude variation. The distribution of wavelet coefficient corresponding to noise occurs just the other way around. Thus, we can get a denoised image simply by screening the estimate of wavelet coefficient through the threshold function and finally reconstructing through the wavelet coefficient. The threshold denoising method is easy to implement and only requires a small amount of calculation. It is widely applied in practice. After threshold processing, the derived processed wavelet coefficient is also relatively intact. Thus, we can reconstruct a wavelet coefficient directly and get a denoised image.

At present, there are two traditional wavelet threshold processing methods, one of which is a hard threshold method, as shown in Eq. 6 below

$$\hat{x} = T_h(x,t) = \begin{cases} x & |x| \geq t \\ 0 & |x| < t \end{cases}. \qquad (6)$$

The wavelet coefficient derived from the hard threshold method has poor continuity. The reconstructed signal may change suddenly or oscillate, as shown in Fig. 3, *a*. Another method is a soft threshold method, which is shown in Eq. 7 below

$$\hat{x} = T_s(x,t) = \begin{cases} x - t & |x| \geq t \\ 0 & |x| > t \end{cases}. \qquad (7)$$

The wavelet coefficient derived from the soft threshold method has good continuity. But when the wavelet coefficient is large, the processed wavelet coefficient will have a certain deviation from the actual wavelet coefficient and lead to an error in the reconstructed result, as shown in Fig. 3, *b* below.

Although soft and hard thresholds have achieved a good effect in practical application, this method itself has some shortcomings. For example, in the hard threshold algorithm, when $x = \pm t$, it is not continuous. So the derived estimated coefficient $\hat{x}$ may be distorted during reconstruction. While for the soft threshold function, when $|x| \geq t$, the derived estimated coefficient $\hat{x}$ has a great deviation from the actual coefficient. Thus, there will be a greater error between a derived image and an actual image after reconstruction. In view of shortcomings of traditional threshold functions, this paper will improve all traditional threshold functions comprehensively. The selected fused traditional threshold function mixes include comprehensive improvement of the fusion of a semi-soft threshold and an eclectic threshold and comprehensive improvement of the fusion of the soft threshold, semi-soft threshold and eclectic threshold. The improve-

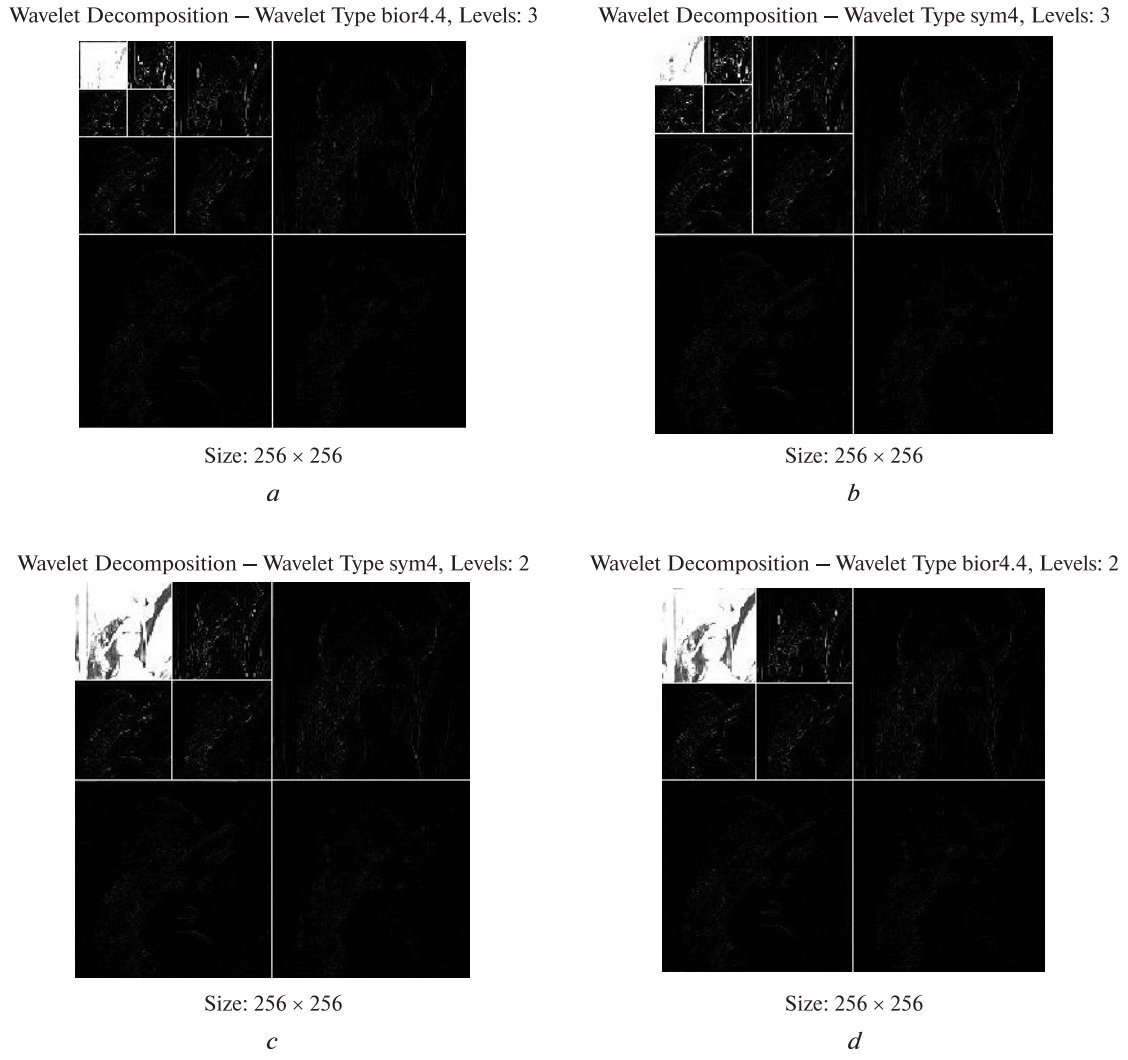

Fig. 2. Image Decomposition Results of Different Wavelet Functions. Fig. 2, a and Fig. 2, b: 3-Level Decomposition Results of Wavelet Functions Bior4 and Sym4; Fig. 2, c and Fig. 2, d: 2-Level Decomposition Results of Wavelet Functions Bior4 and Sym4

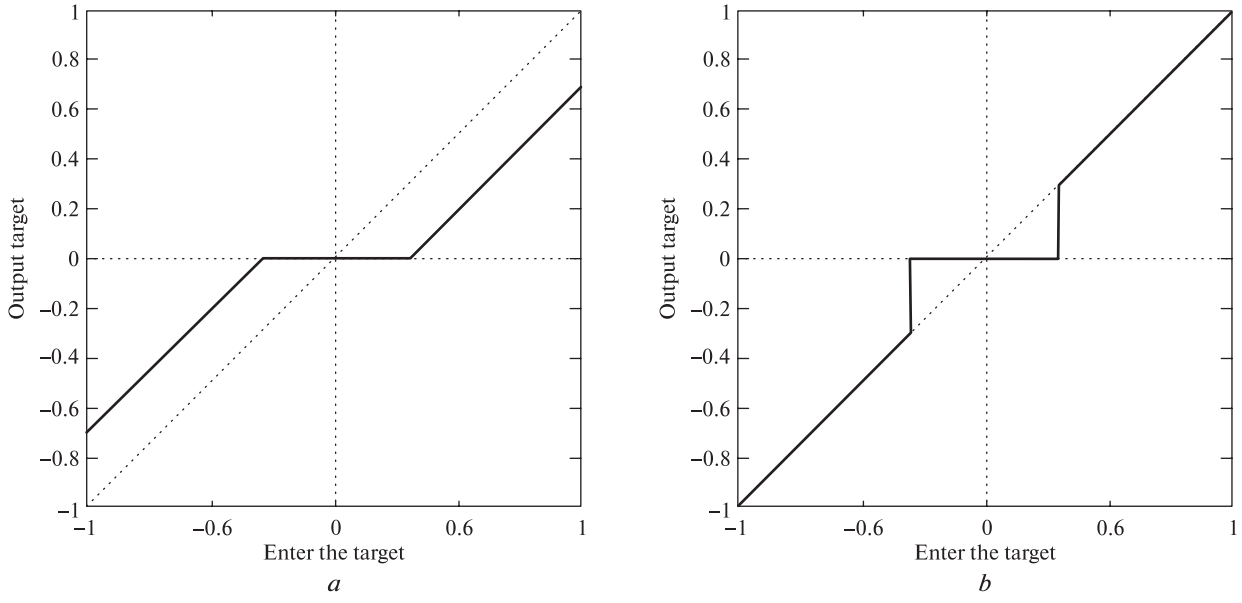

Fig. 3. Two Traditional Threshold Functions:
a — Soft Threshold Function; b — Hard Threshold Function

ments of above fusion threshold functions are referred to Fusion Threshold Function A and Fusion Threshold Function B respectively, as shown in Eq. 8 and 9

$$\hat{x} = T(x,t) = \begin{cases} \operatorname{sgn}(x)\cdot\dfrac{tmp1+|tmp1|}{2} & |x|\geq t \\ \operatorname{sgn}(x)\cdot\dfrac{(t-at)(tmp+|tmp|)}{2(t-t_0)} & |x|<t \,\&\, |x|>t_0 \end{cases}. \quad (8)$$

Where $tmp = |x| - t_0$, $tmp1 = |x| - at$, a is the control factor and $0 < a < 1$.

$$\hat{x} = T(x,t) = \begin{cases} \operatorname{sgn}(x)\cdot\dfrac{|x|-2kt}{(k+0.5)\lambda} & |x|\geq t \\ \dfrac{kx^{2k+1}}{(2k+1)t^{2k}} & |x|<t \end{cases}. \quad (9)$$

Where $\lambda = 1 + e^{\left(\frac{|x|}{2}-\frac{t}{2}\right)}$, generally let $k = 2$.

All threshold functions established above fuse the advantages of traditional threshold functions. Thus they can effectively overcome the shortcomings of discontinuity in hard threshold and constant deviation in soft threshold. All fusion threshold functions are shown in Fig. 4 below.

Wavelet Transformation Image Denoising Procedures Based on Fusion Threshold Functions.

Step 1: To decompose an image with noise into N levels using the wavelet 'wname'. The approximate detail coefficient C and the width L corresponding to the detail coefficient of image transformation are obtained.

Step 2: To get a preset threshold of the fixed threshold function using the *VisuShrink* threshold method. To process the threshold function of the image approximate detail coefficient C derived from Step 1 and obtain the image approximate detail coefficient after the threshold function processing.

Step 3: To completely reconstruct the image approximate detail coefficient after processing the threshold function derived from Step 2 and the width L corresponding to the detail coefficient derived from Step 1 at a single time using 'wname' and obtain a denoised image.

Step 4: To calculate the mean square error (MSE), root mean square error (RMSE), peak signal-to-noise ratio (PSNR) and signal to noise ratio (SNR) between the denoised image and original image and then evaluate the denoising effect. The smaller indices MSE and RMSE are, the better, while the bigger indices PSNR and SNR are the better.

Image denoising experiment result analysis. In order to validate the denoising effect of the proposed fusion threshold functions in this paper, the author compares denoising between fusion threshold functions and traditional threshold functions.

In the process of image denoising experiment, by adding Gaussian noise with the value of $u = 0$ and the variance of $\sigma = 20$ artificially, meanwhile considering the amount of calculation and denoising effect of algorithm in the process of wavelet decomposition, the wavelet function "db8" is selected for decomposition. Supposing that the number of wavelet decomposition levels is 3 let the control coefficient of fusion threshold function be 0.1. "Lena" image, which is 512×512 in size and 256 in grey scale, is used as an analysis object of the model denoising experiment. The original image and imnoised image are shown in Fig. 5 below.

The image approximation coefficient derived from "db8" wavelet function decomposition and approximation coefficients after processing with all threshold functions are shown in Fig. 6 below. The derived denoising results are shown in Fig. 7 below.

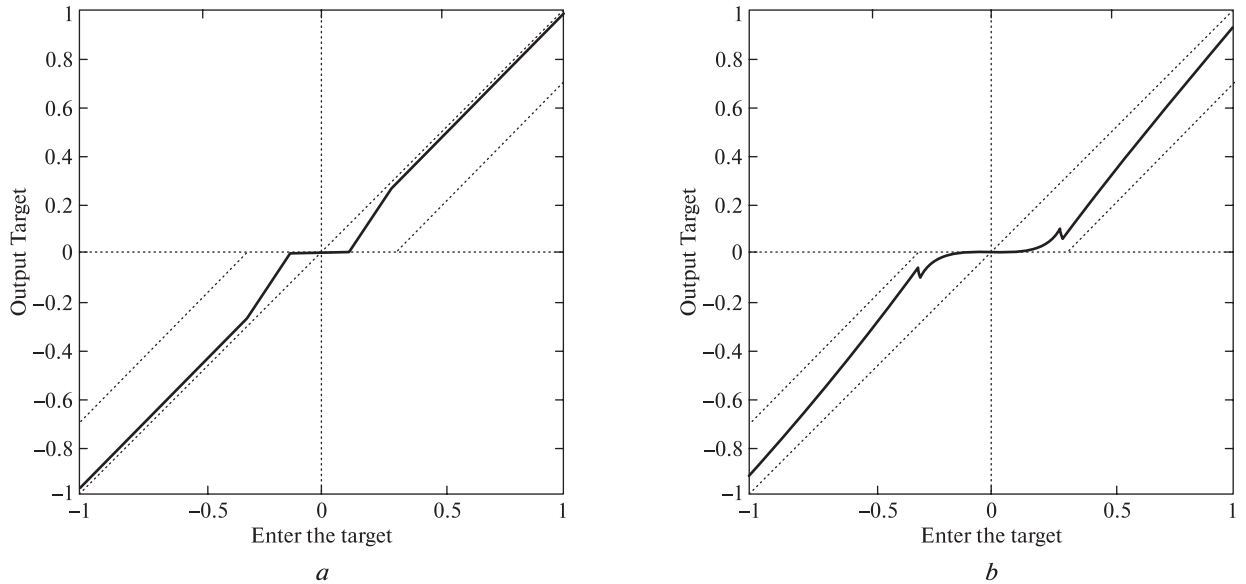

a *b*

Fig. 4. Two Fusion Threshold Functions:
a — Fusion Threshold Function A; b — Fusion Threshold Function B

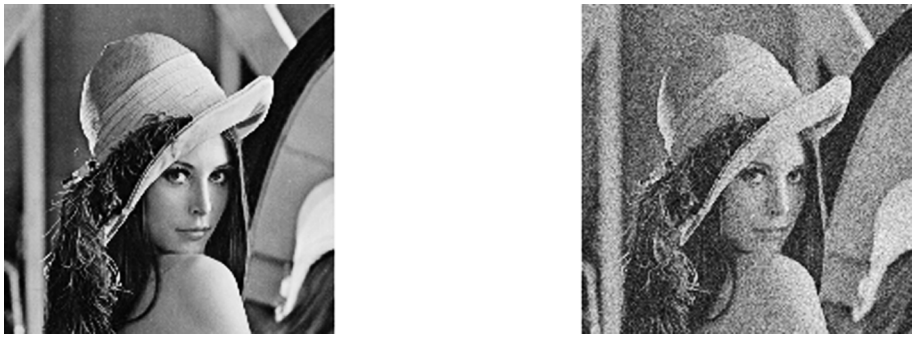

a *b*

Fig. 5. Experimental Lena Images:

a — Original Image; b — Imnoised Image

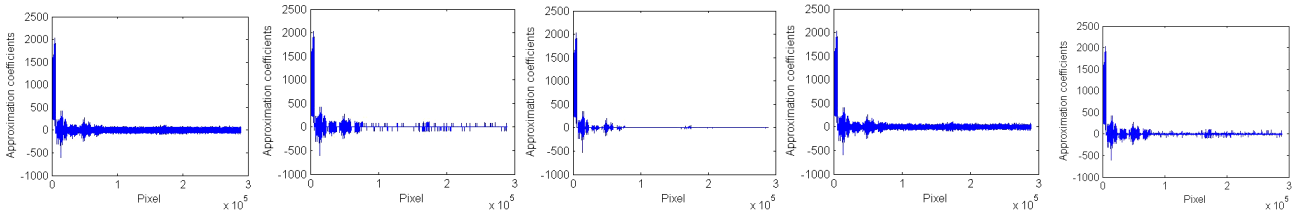

a *b* *c* *d* *e*

Fig. 6. Image Approximation Coefficients after Processing with All Threshold Functions:

a — Approximation Coefficient Derived from Wavelet Decomposition; b — Hard Threshold Processing Results; c — Soft Threshold Processing Results; d — Processing Results of Fusion Threshold A; e — Processing Results of Fusion Threshold B

a *b*

c *d*

Fig. 7. Denoising Results of All Threshold Functions:

a — Hard Threshold Denoising Results; b — Soft Threshold Denoising Results; c — Denoising Results of Fusion Threshold A; d — Denoising Results of Fusion Threshold B

From the results in Fig. 6 above, we can see that the estimated wavelet threshold coefficient derived from the hard threshold function processing has a certain discontinuity, while the soft threshold processing results are too smooth. The details of the image may be lost easily. For Fusion Threshold Functions *A* and *B*, continuity and smoothness have been taken into account when estimating the wavelet coefficient, so the characteristics of discontinuity and over-smoothness have not emerged.

It can be seen from Fig. 7 above that hard threshold denoising can better retain the edge details of an image, but oscillation will occur. Soft threshold denoising has a smooth effect, but the processing of the edge details is inferior to that of the hard threshold. The overall feeling is fuzzy. On the other hand, Fusion Threshold Functions *A* and *B* do not only retain the edge details of an image, but also achieve a smooth effect. Compared with traditional threshold functions, they improve distortion and oscillation favourably. The relevant denoising evaluation indices of all threshold functions are shown in Table below. From the denoising evaluation index results below, we can see that Fusion Threshold Functions A and B have a better denoising effect than traditional threshold functions.

Conclusions. This paper first analyses the image transformation process of two-dimensional wavelet decomposition, takes an image approximation coefficient derived from two-dimensional wavelet decomposition as the basis of extraction and analyses the structures and defects of traditional threshold functions. According to the characteristics of traditional threshold functions and basic design ideas and procedures, it presents two fusion threshold functions based on traditional threshold functions and gives a simulation diagram of corresponding threshold function extraction. Through the simulation diagram of the threshold function, it can be seen that fusion threshold functions integrate advantages of traditional threshold functions, overcome the discontinuity of the hard threshold function and constant deviation in the soft threshold function. Finally, with "Lena" image, which is 512×512 in size and 256 in grey scale, as an example, by imnoising corresponding Gaussian noise artificially, the author denoises the image with all threshold functions. The results show that the proposed fusion threshold function algorithms in this paper can retain all details in images apart from removing noises in images effectively. By calculating relevant denoising evaluation indices, compared with traditional threshold functions, the fusion threshold functions have improved all denoising evaluation indices.

References/Список літератури

1. Mo X. Q. and He A., 2014. Engineering Image Processing Based on Adaptive Threshold Median Filtering Algorithm. *Software Guide*, No. 3, pp. 55–59.
2. Xu S. S., 2015. *The Application of Improved Fuzzy C-Means Clustering Algorithm in Image Segmentation*. Chang'an University.
3. Liu D. J., 2013. Research on Image Denoising Method in Image Edge Detection.*Computer CD Software and Applications*, No. 12, pp. 303–303.
4. Sun X. X. and Qu W., 2014. Comparison between Mean Filter and Median Filter Algorithm in Image DenoisingField". *Applied Mechanics & Materials*, pp. 4112–4116.
5. Zhang X., Feng X. and Wang W., 2013. Gradient-based Wiener filter for image denoising. *Computers & Electrical Engineering*, Vol. 39, No. 3, pp. 934–944.
6. Li T. K., Liu H. and Wang, 2013. Self-adaptive Kalman Filter Algorithm Research Based on Wavelet Transform. *Ordnance Industry Automation*, No. 1, pp. 32–35.
7. Xing W. L. and Zhang B. H., 2014. An Improvement Based on Wavelet Transform Speech Denoising Threshold Function. *Advanced Materials Research*, pp. 828–832.
8. Hu Y. H., 2015. *Compressed Sensing Image Denoising Method and its Application in Wireless Decay Channels*. East China Jiaotong University.

Мета. У зв'язку з існуванням характерних постійних девіацій і розривності шумоподавляючої порогової функції вейвлета, у роботі аналізуються можливості нової шумозаглушуючої функції в результаті інтеграції традиційних вейвлетних порогових функцій.

Методика. Шляхом аналізу недоліків м'якої порогової функції та жорсткої порогової функції вейвлета, згідно з характеристикам традиційної порогової функції, а також задуму й процедурі розробки, робота встановлює інтегровану порогову функцію на основі традиційної порогової функції та пропонує схему моделювання, що вилучена з відповідної порогової функції. За допомогою схеми моделювання порогової функції, у роботі аналізуються переваги інтегрованої порогової функції.

Table

Denoising Effect of Different Threshold Functions ($u = 0$, $\sigma = 20$)

Threshold Function	MSE	RMSE	PSNR	SNR
Original Image with Noise	400.7895	20.0197	22.1016	16.4453
Hard Threshold Function	86.0618	9.2770	28.7827	27.5931
Soft Threshold Function	113.1806	10.6386	27.5931	21.9367
Fusion Threshold Function A	89.9547	9.4844	28.5906	22.9342
Fusion Threshold Function B	74.9180	8.6555	29.3849	23.7286

Результати. Згідно з результатами, інтегрована порогова функція, встановлена на основі м'якої й жорсткої порогових вейвлетних функцій, об'єднує переваги традиційних порогових функцій, ефективно долаючи розривність жорсткої порогової функції та девіації м'якої порогової функції.

Наукова новизна. У ході дослідження фільтрації шуму вейвлетної порогової функції встановлено, що попередні дослідження використовували традиційні порогові функції для проведення операції прямої деформації, але нехтували перевагами традиційної порогової функції вейвлета. Завдяки характеристикам і ідеям традиційної вейвлетної порогової функції, робота об'єднує традиційні вейвлетні м'яку й жорстку порогові функції, що забезпечує операцію деформації та здібність до самоадаптації.

Практична значимість. Отриманий у роботі результат дозволяє ефективно покращувати здатність фільтрації шумів зображення, що не лише може ефективно видаляти шум, але й також зберігати детальну інформацію зображення, закладаючи міцну основу для поглибленої обробки високоякісного зображення.

Ключові слова: *вейвлет-перетворення, порогова функція, порогова функція злиття, шумозаглушення зображення*

Цель. В связи с существованием характерных постоянных девиаций и разрывности шумоподавляющей пороговой функции вейвлета, в работе анализируются возможности новой шумоподавляющей функции в результате интеграции традиционных вейвлетных пороговых функций.

Методика. Путём анализа недостатков мягкой пороговой функции и жесткой пороговой функции вейвлета, согласно характеристикам традиционной пороговой функции, а также замыслу и процедуре разработки, работа устанавливает интегрированную пороговую функцию на основе традиционной пороговой функции и предлагает схему моделирования, извлеченную из соответствующей пороговой функции. Посредством схемы моделирования пороговой функции, в работе анализируются преимущества интегрированной пороговой функции.

Результаты. Согласно результатам, интегрированная пороговая функция, установленная на основе мягкой и жесткой пороговых вейвлетных функций, объединяет преимущества традиционных пороговых функций, эффективно преодолевая разрывность жесткой пороговой функции и девиации мягкой пороговой функции.

Научная новизна. В ходе исследования фильтрации шума вейвлетной пороговой функции установлено, что предыдущие исследования использовали традиционные пороговые функции для проведения операции прямой деформации, но пренебрегали преимуществами традиционной пороговой функции вейвлета. Благодаря характеристикам и идеям традиционной вейвлетной пороговой функции, работа объединяет традиционные вейвлетные мягкую и жесткую пороговые функции, что обеспечивает операцию деформации и способность к самоадаптации.

Практическая значимость. Полученный в работе результат позволяет эффективно улучшать способность фильтрации шумов изображения, что не только может эффективно удалять шум, но также сохранять детальную информацию изображения, закладывая прочное основание для углубленной обработки высококачественного изображения.

Ключевые слова: *вейвлет-преобразование, пороговая функция, пороговая функция слияния, шумоподавление изображения*

Рекомендовано до публікації докт. техн. наук В. В. Гнатушенком. Дата надходження рукопису 27.05.15.